 doi:10.20944/preprints201808.0085.v2

Research Article

Experimental Investigation of Impact Detection and Damage Extent Quantification

Mohammad Faisal Haider [1,*], Asaad Migot [1], Md Yeasin Bhuiyan [1] and Victor Giurgiutiu [1]

[1] Department of Mechanical Engineering, University of South Carolina, 300 Main Street, Columbia, SC 29208
* Correspondence: haiderm@e-mail.sc.edu; Tel.: +1-803-777-0619

Abstract: This paper focused on impact localization of composite structures, which possess more complexity in the guided wave propagation because of the anisotropic behavior of composite materials. In this work, a composite plate was manufactured by using a compression molding process with proper pressure and temperature cycle. Eight layers of woven composite prepreg were used to make the plate. A structural health monitoring (SHM) technique is implemented with piezoelectric wafer active sensors (PWAS) to detect and localize the impact on the plate. There are two types of impact event are considered in this paper (a) low energy impact event (b) high energy impact event. Two clusters of sensors recorded the guided acoustic waves generated from the impact. The acoustic signals are then analyzed using a wavelet transform based time-frequency analysis. The proposed SHM technique successfully detect and localize the impact event on the plate. The experimentally measured impact locations are compared with the actual impact locations. An immersion ultrasonic scanning method was used to visualize the composite plate before and after the impact event. A high frequency 10 MHz 1-inch focused transducer was used to scan the plate in an immersion tank. Scanning results show that there is no visible manufacturing damage in the composite plate. However, clear impact damage was observed after the high-energy impact event.

Keywords: impact localization, composite materials, PPS, imaging method, immersion ultrasonic scanning

1. Introduction

Advanced composites are increasingly being used in many applications [1–4]. However, the prognosis of their long-term behavior is still an active area of research. The ability to predict functional life depends upon characterizing and predicting the evolution of the material state of the structure (e.g., distributed damage development, accumulation, and interaction) which affect global property (strength and stiffness) degradation and eventual failure. The lack of monitoring of that local damage often results in empiricism, limiting innovation in the use of composite materials. Therefore, appropriate nondestructive inspection (NDI) and structural health monitoring (SHM) technique is in urgent need for composites structure [5–7]. The maintenance costs associated with the aging infrastructure becoming an ongoing concern. In addition to maintenance cost, downtime of those structures makes the economy more inviable. SHM may alleviate this economy barrier by (a) assessing the state of the structure beforehand and do the on-site maintenance with minimum downtime and (b) ensuring increased safety and reliability while reducing maintenance costs. For new structures, the embedded sensors and sensing systems from the design stage are likely to reduce the overall life-cycle cost. [8]. SHM has been implemented for composites using a built-in sensor network [8,9] and real-time pipeline integrity monitoring [11].

The acoustic events can be from many different sources such as (a) impact of a foreign object (bird strike, debris hit) [12] (b) fatigue crack generation in the structures [13], (c) matrix cracking, fiber breakage and/or delamination of the composites. The detection, localization, and sizing of the

 doi:10.20944/preprints201808.0085.v2

damage from all these events is an essential area of SHM [14–16]. These acoustic events mostly generate the waves in an ultrasonic regime [17]. These waves propagate in the structures and carry the information of the acoustic events. Now the research question is: how can one capture these waves and extract damage-related information?

Undetected impact damage has a long track record of causing severe failure to composite structures. The impact damage from airport debris caused Concord to fly miserably and led to disaster. Hitting by debris or any foreign object is very common for moving structures, and after any such hit, the structure should be adequately inspected especially near the impact location. Therefore, this impact location must be identified by an appropriate acoustic source localization method. After identifying the impact region, a more careful active SHM can be performed to conclude the severity of the damage caused by such impact [18,19]. Active SHM has been implemented to quantify the damage [20], and a non-contact approach has been implemented in pipeline defects [21]. However, these research mainly focused on aluminum alloys.

In this research, a comprehensive study has been carried out starting from the manufacturing the composite plate to final impact detection and localization using SHM approach. A composite plate was manufactured from woven carbon fabric prepreg by using a compression molding process. An SHM technique has been implemented to detect and localize the impact event by using permanently bonded piezoelectric wafer active sensors in the manufactured composite plate. We found that the experimental measurements are in good agreement with actual impact localization. The manufactured composite plate was tested nondestructively using immersion ultrasonic scanning. The scanning results showed that the plate had a minimal to no manufacturing defect that can affect the impact detection and localization.

2. Composite plate manufacturing using compression molding process

Polyphenylene Sulfide (PPS) fabric prepreg (TC1100) from TenCate Cetex was used to manufacture the thermoplastic composite (TPC) plate. The PPS prepreg was a pre-consolidated reinforced laminate with continuous woven carbon fibers. TC1100 is pre-consolidated reinforced laminate (RTL) utilizing continuous woven carbon fibers (Carbon T300 3K).

Figure 1. Composite layers (a) with thin protective films (b) in the compression-molding machine

The prepreg was cut to the desired shape (square in this case) with a dimension of 305 mm by 305 mm (12 inches by 12 inches). Each cutting section served as a layer. Eight layers of woven fabric then stacked upon each other to form a laminate. Two thin protective films of plastics with a very high melting point were used on top and bottom of the stack up (**Figure 1** a)). The laminate of eight layers was then placed between two flat platens of the compression-molding machine as shown in **Figure 1**(b). The melting temperature of the PPS fabric is 536 0F. Hence, a cure cycle must contain a

Preprints (www.preprints.org) | NOT PEER-REVIEWED | Posted: 7 August 2018 doi:10.20944/preprints201808.0085.v2

temperature higher than the melting point for proper melting and flow of the resin. **Figure 2** (a) shows a standard cure cycle used for this laminate. A constant pressure of 150 psi was applied during the cure cycle. Heating was adjusted in the compression-molding chamber for raising the laminate temperature to 610 0F within 45 minutes. Then the temperature of the laminate dwelled at 610 0F for 30 minutes. At the end of dwell time, the laminate was air cooled from 610 0F to room temperature in 30 minutes. After the cure cycle completed in about 2 hours, the laminate was taken out from the platen. The extra resin flow at the edges of the laminate was trimmed. **Figure 2** (b) shows the final composite laminate after the trimming process. The resulting plate had a thickness of 1.6-mm. The dimension of the final composite plate was 387 mm by 276 mm (11.3 inches by 10.9 inches).

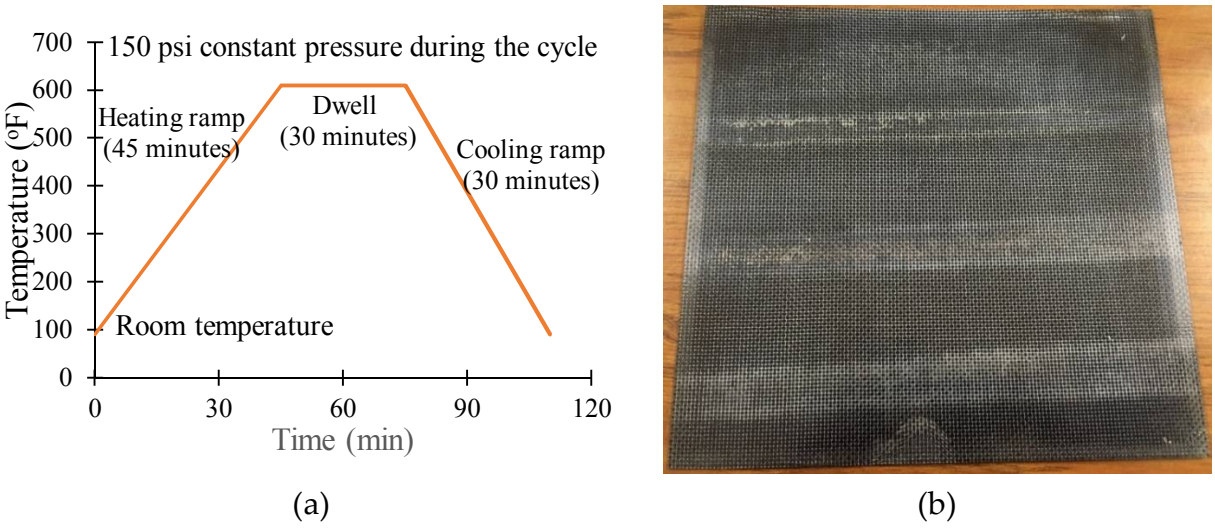

Figure 2. (a) Cure cycle for the PPS prepreg (b) Final composite plate

3. Impact detection and localization using SHM technique

The impact is a common damage situation that can occur in real-life structures. In this experiment, a structural health monitoring (SHM) technique is implemented to detect and localize the impact. Six lead zirconate titanate (PZT) piezoelectric wafer active sensors (PWAS) are permanently bonded to the composite plate. Each PWAS transducer is 7-mm in diameter and 0.5-mm in thickness.

3.1. Developing Imaging method

To localize the impact point in the interested area, we divided it into the small pixel. There are two intersected lines for every cluster [23]. In this method, two-lines paths are mapped from each clusters and intersected at the impact location as shown the **Figure 3**. The flow chart of the developed imaging method is illustrated in **Figure 4**. The first step in this imaging approach, we determine the slope values for every clusters based on the time of flight of clusters sensors as follow

$$\text{Slope}^1 = \frac{\Delta t_{23}}{\Delta t_{21}}$$
$$\text{Slope}^2 = \frac{\Delta t_{56}}{\Delta t_{54}} \quad (1)$$

Where Slope^1 and Slope^2 are slope values of Cluster1 and Cluster2. Δt_{23} is the difference in time of flight between sensors S_2 and S_3.

Preprints (www.preprints.org) | NOT PEER-REVIEWED | Posted: 7 August 2018 doi:10.20944/preprints201808.0085.v2

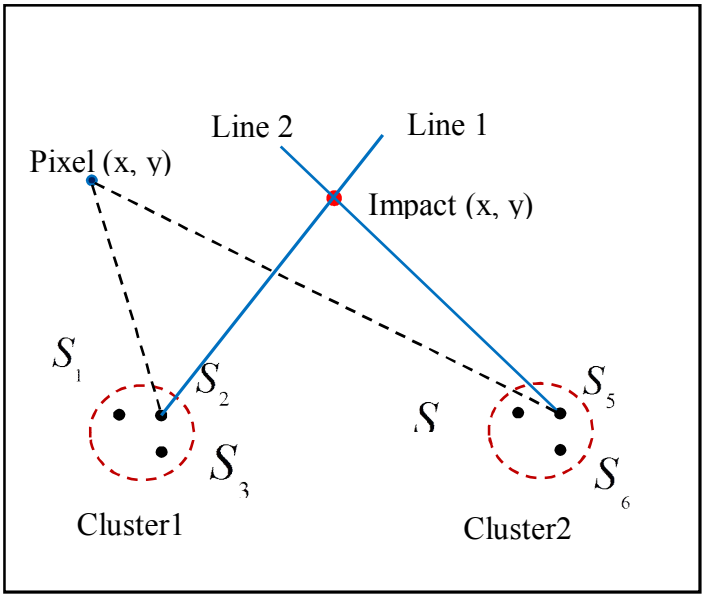

Figure 3. Mapping of two lines from each cluster to show the intersection at the impact location

The second step, we determine the slope values for every pixel of the interested area for a particular sensing path line of a particular cluster as follow

$$\text{Slope}_{ij}^{\ 1} = \frac{y_2 - y_i}{x_2 - x_j}$$

$$\text{Slope}_{ij}^{\ 2} = \frac{y_5 - y_i}{x_5 - x_j} \quad (2)$$

where $(x_2, y_2), (x_5, y_5)$ are the coordinates of sensors S_2 (in Cluster1) and S_5 (in Cluster2) respectively. To determine the pixels field values for every individual path, we use Gaussian distribution equation

$$f_{ij}^{k}(x, y) = \frac{1}{\sigma\sqrt{2\pi}} e^{-\frac{(x-\mu)^2}{2\sigma^2}} \quad (1)$$

where $f_{ij}^{k}(x, y)$ is the field value of every pixels $P(x, y)$ of the image for a particular sensing path line (for a particular cluster), x represents the slope value at each pixels $Slope_{ij}^{\ k}$ for the sensing path line of $Cluster\,k$, μ represents the slope value for the sensing path line of $Cluster\,k$ which can be determined experimentally based on the time of flight values of cluster sensors. The standard deviation, σ which describes the variability or dispersion of a data set, which was taken as a function of slope value. In this work, the σ values were taken between 0.02-1. k represents the order of used cluster.

To fuse all the images from different sensing paths, summation and/or multiplication algorithm were used [10,24] following the equations below:

Preprints (www.preprints.org) | NOT PEER-REVIEWED | Posted: 7 August 2018 doi:10.20944/preprints201808.0085.v2

$$P_{sum}(x,y)=\sum_{k=1}^{N} f_{ij}^{k}(x,y)$$
$$P_{mult}(x,y)=\prod_{k=1}^{N} f_{ij}^{k}(x,y) \quad (2)$$

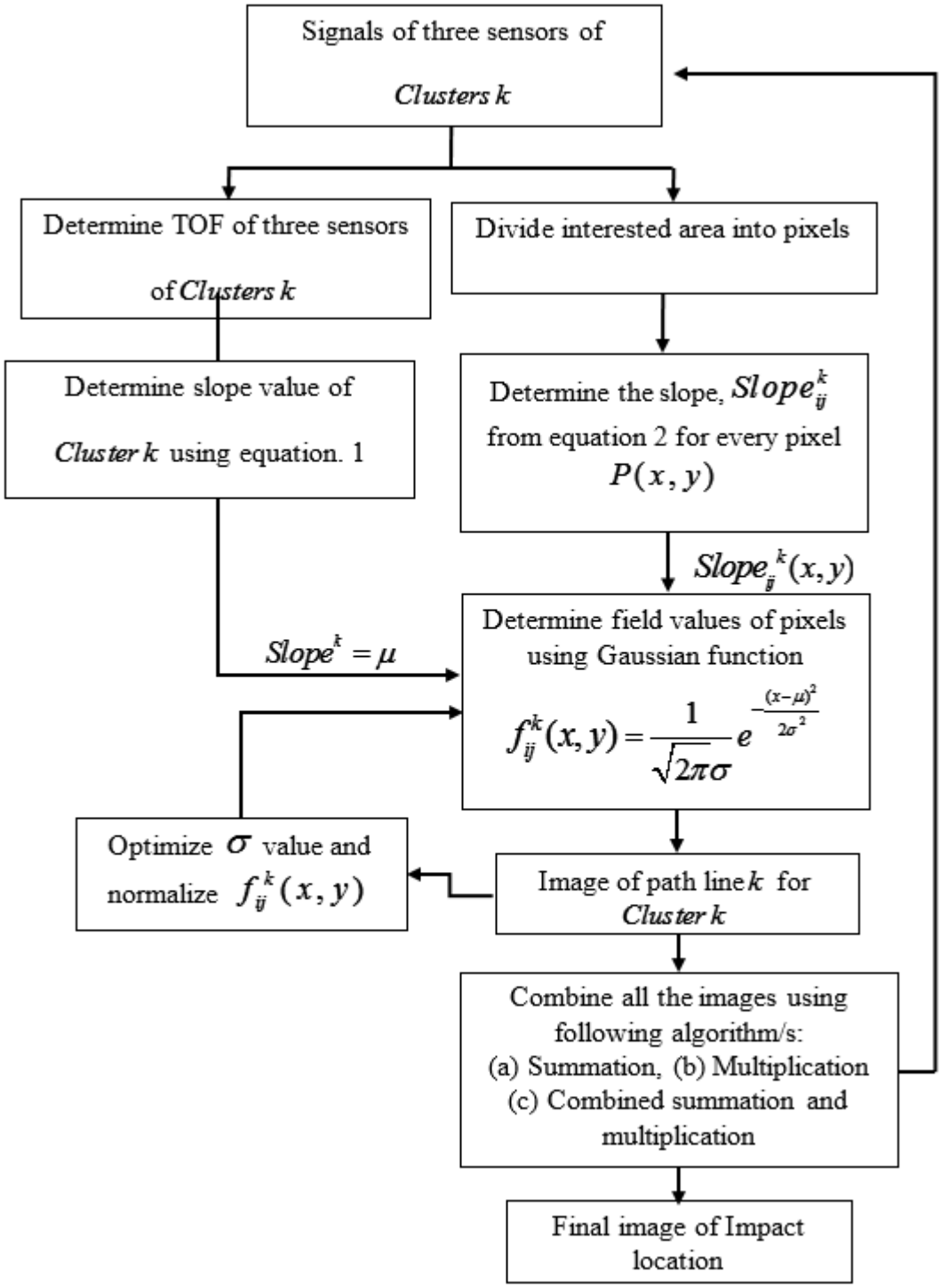

Figure 4. Flowchart of the developed imaging method

where $P_{sum}(x,y), P_{mult}(x,y)$ are the total field values of each pixels using a summation or multiplication algorithm. N represents the total number of sensing paths lines which equal to the

Preprints (www.preprints.org) | NOT PEER-REVIEWED | Posted: 7 August 2018 doi:10.20944/preprints201808.0085.v2

total number of clusters. In this work, we have used two clusters. **Figure 4** shows the details procedure of imaging method.

3.1 SHM experimental setup for impact detection and localization

The experimental setup is shown in **Figure 5**. Two clusters of PWAS sensors were used as named Cluster1 (at coordinate location (60, 53)) and Cluster2 (at coordinate location (197, 53)). In each cluster, there were three PWAS transducers placed at 90 deg. Orientation. These configuration of sensors are especially useful when one does not know the exact material properties of the plate. This method can accurately predict the location of the impact by analyzing the received signals by the sensors without knowing the material properties. Signals from an impact location were received through six sensors using two oscilloscopes (**Figure 5**).

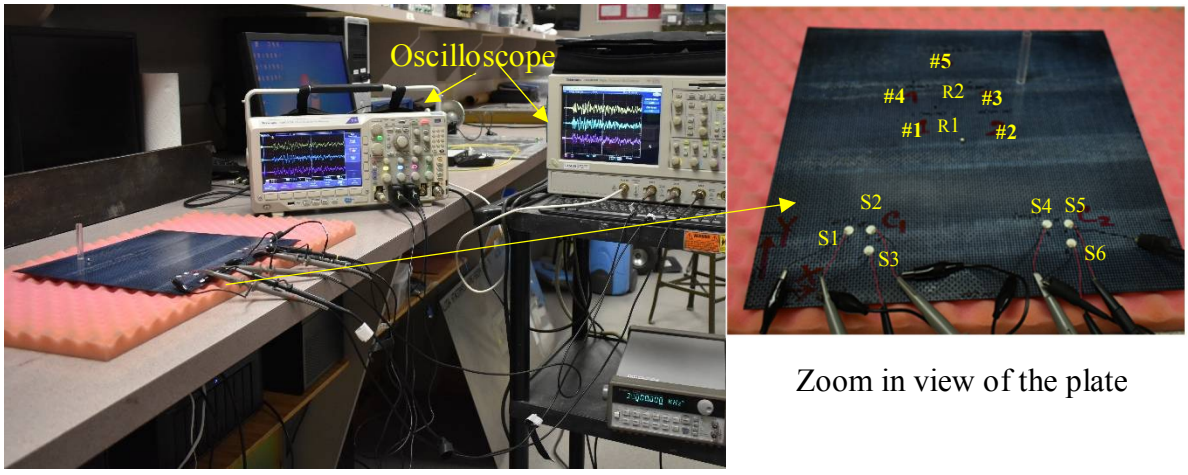

Figure 5. Experimental setup for impact detection and localization on the composite plate

3.2 Low-energy impact method

The plate was subjected to impact by a steel ball at five different locations. These locations are marked by #1, #2, #3, #4, and #5 in **Figure 5**. At each location, three impact events were created to check the repeatability of the test. The steel ball was freely impact following a special guide fixture from a height of about 2 inches. When the steel ball hit the plate, it generates acoustic emissions. The energy of acoustic emission (AE) propagates as guided waves in the plate. The guided waves produce stress and strain waves in a plate. The permanently bonded PWAS transducers captured the strain waves. Since the six PWAS transducers were located at different distances, the time of flights (TOF) of the received signals was different.

3.2.1. Experimental Signal Analysis and Impact Detection

The six signals from the six sensors are illustrated in **Figure 6**. **Figure 6** corresponds to the signals received from impact location#3. Only the low-energy impact at location #3 is presented here as a representative result. These signals received by the sensors indicate that there was an impact event. In this experiment, low energy impact (height was intentionally kept low) was used to show how sensitive the proposed SHM system is. In case of high energy impact, it would be much easier to detect the impact event since it would produce higher amplitude AE signals.

Preprints (www.preprints.org) | NOT PEER-REVIEWED | Posted: 7 August 2018 doi:10.20944/preprints201808.0085.v2

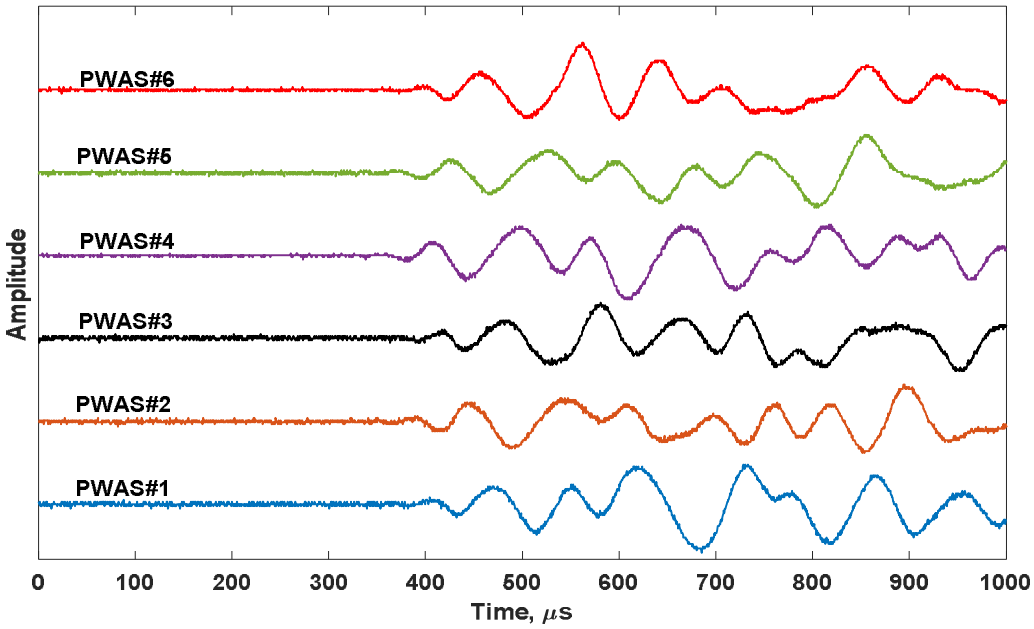

159

160 **Figure 6.** PWAS recorded acoustic signals due to low-energy impact at location #3 (150, 200) mm

161 3.2.2. Low-energy impact Localization

162 To localize the impact event in the plate, it is essential to determine the time-of-flight correctly.
163 Just by looking at the time-domain signals, often it is hard to determine the time of flight. The accurate
164 way is to use a signal processing method to determine TOF. A wavelet transform based method was
165 used in this paper to determine the TOF. The wavelet transform based method is demonstrated in
166 **Figure 7**. As an example, two PWAS signals received from impact event # 3 are considered.

Preprints (www.preprints.org) | NOT PEER-REVIEWED | Posted: 7 August 2018 doi:10.20944/preprints201808.0085.v2

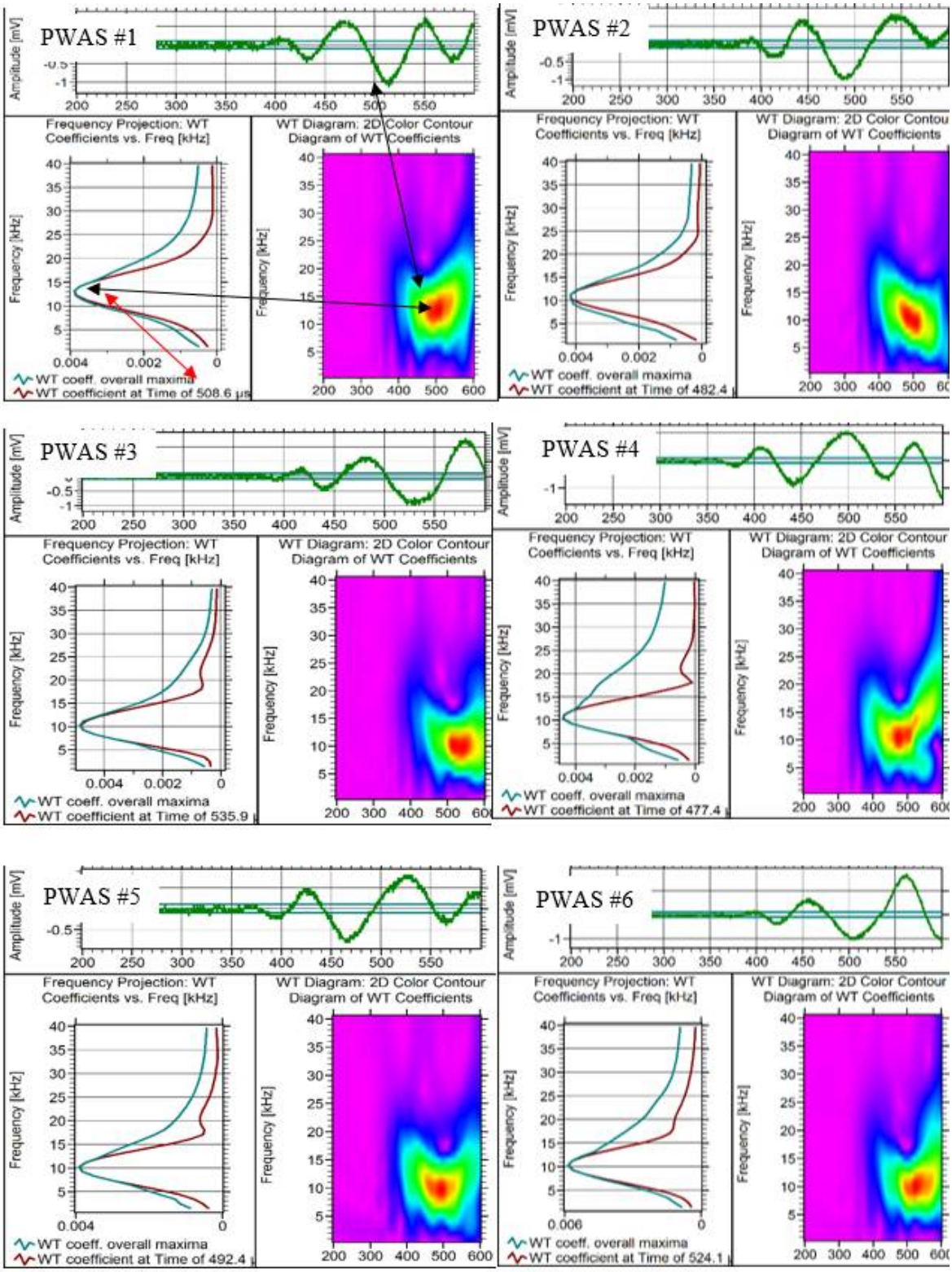

Figure 7. Wavelet transform of the PWAS recorded signals to determine time of flight (TOF) (for low-energy impact location #3)

In wavelet transform (WT), adjustable windows can better keep track of time and frequency information as compared to short-time Fourier transform (STFT), another popular method. WT can zoom in on short bursts and zoom out to detect long, slow oscillations by auto adjustment of the windows. Since the nature of the signal is unknown during an impact, WT provides more accurate information from the time-frequency analysis. A freeware Vallen software [25] was used to perform WT on the signals. This program has a Gabor function as the "mother" wavelet.

Preprints (www.preprints.org) | NOT PEER-REVIEWED | Posted: 7 August 2018 doi:10.20944/preprints201808.0085.v2

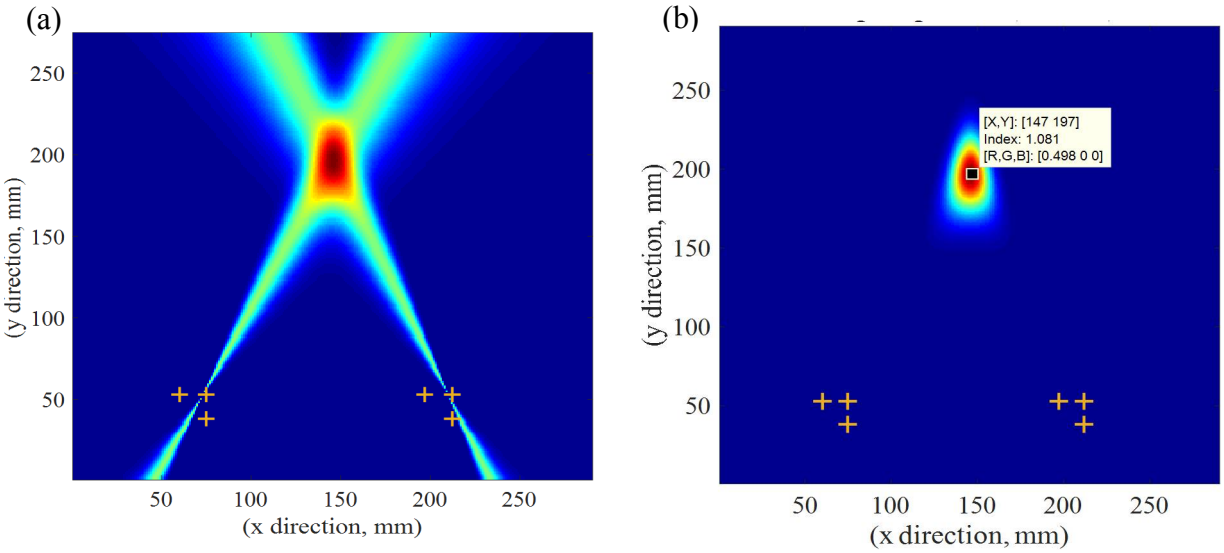

Figure 8. Imaging results of localization low-energy impact at point #3 (150, 200) mm using imaging methods; (a) summation method; (b) multiplication method

Table 1 Experimental measurement vs. actual location of the low-energy impact

Impact event	Actual location (x, y) mm	Measured location (x, y) mm	% of error (Based on sensor cluster 1)
#1	(120, 170)	(117.7, 161.9)	6.7%
#2	(170, 170)	(166, 163.8)	4.8%
#3	(150, 200)	(147.4, 197.8)	1.9%
#4	(100, 200)	(101.8, 195.5)	2.7%
#5	(130, 250)	(131.7, 251.6)	0.9%

The WT diagrams in **Figure 7** show the frequency-time plot using the WT. It shows the amplitude mapping over various frequencies and time. At each time and frequency, a WT coefficient variation can be plotted as shown on the bottom-left of each box. An overall maximum of the WT coefficient has been plotted. The time at which the WT profile matches the overall WT maxima provide the TOF. This process has been repeated for all PWAS signals to determine the TOFs.

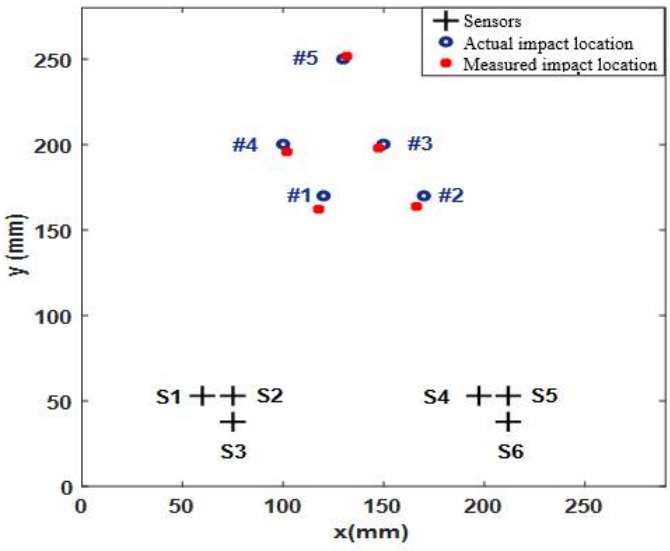

Figure 9. Experimentally measured low-energy impact location and actual impact location on the manufactured composite plate

 doi:10.20944/preprints201808.0085.v2

Once the TOFs for all the AE signals were known, a localization algorithm was used to determine the impact location. The imaging method is described in earlier section (Section 3.1). The results from the imaging method is illustrated in **Figure 8**. The experimental measurement and the actual impact location is summarized in **Table 1**. The visual representation of the actual impact location and measured impact location is shown in **Figure 9.**Experimentally measured low-energy impact location and actual impact location on the manufactured composite plate. It shows that the experimentally measured impact locations are in good agreement with the actual impact location.

3.3 High-energy impact method

In this section impact localization was done due to high energy impact. The plate was subjected to impact by a sharp point cylinder at two different locations. These locations are marked by R1 and R2. The sharp point cylinder was freely impact following a special guide fixture to create 9J impact energy. The six signals from the six sensors are illustrated in **Figure 10**. **Figure 10** corresponds to the signals received from impact location R1.

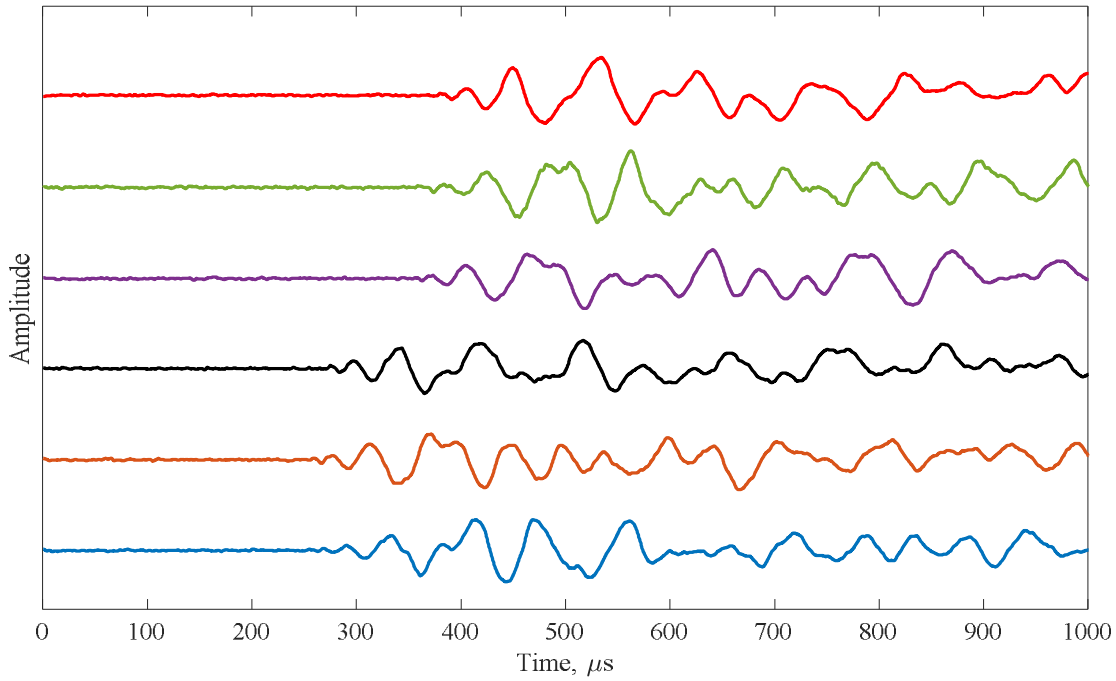

Figure 10. PWAS recorded acoustic signals due to high-energy impact at location #R1 (128, 167 mm)

A wavelet transform based method was used to determine the TOF as described in the previous section (section 3.2.2).**Figure 11** illustrates the impact location of high-energy impact using developed imaging method. The experimental measurement and the actual impact location is summarized in Table 2. It can be observed from Table 2 that the impact location determined by the current approach is very accurate compared to the actual impact location.

Preprints (www.preprints.org) | NOT PEER-REVIEWED | Posted: 7 August 2018 doi:10.20944/preprints201808.0085.v2

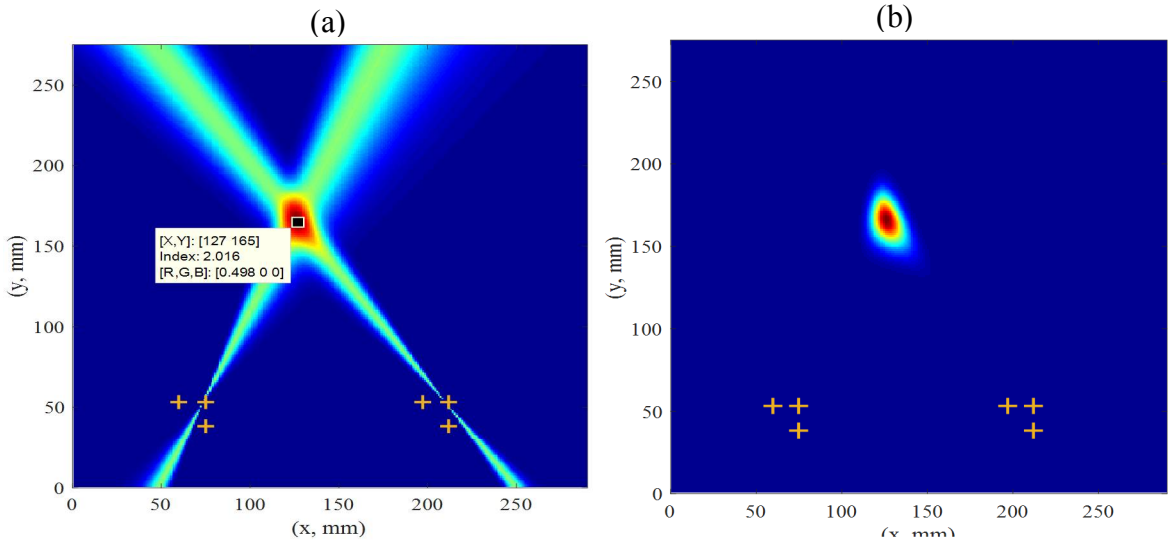

Figure 11. Imaging results of localization high-energy impact at point #R1 (128, 167) mm using imaging methods; (a) summation method; (b) multiplication method

Table 2 Experimental measurement vs. actual location of the high-energy impact

Impact event	Actual location (x, y) mm	Measured location (x, y) mm	% of error (Based on sensor cluster 1)
#1	(128, 167)	(125, 165)	2.4%
#2	(147, 207)	(146, 204)	2.8%

4. Nondestructive inspection (NDI) of the composite plate using immersion ultrasonic testing

An ultrasonic nondestructive inspection (NDI) was performed on the manufactured composite plate before and after the impact event. The purpose of this NDI was to verify if there is any major flaws, delamination or defects during the manufacturing process and to visualize the damage after the impact. An immersion ultrasonic scanning was performed on the plate, which can detect defects or delamination across its thickness. The ultrasonic immersion tank is used to inspect the composite specimen. This device can be used to identify the internal porosity, detect and size of delamination and other types of defects.

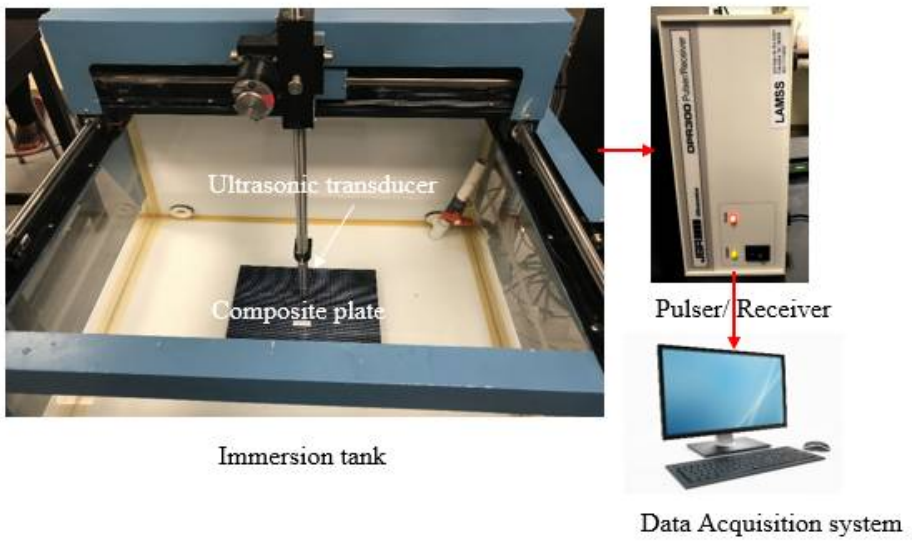

Figure 12. Experimental setup for the ultrasonic inspection of stiffened plate under water

Preprints (www.preprints.org) | NOT PEER-REVIEWED | Posted: 7 August 2018 doi:10.20944/preprints201808.0085.v2

In immersion testing, the transducer is placed in the water, above the test object, and a beam of sound is projected. The experimental setup of immersion ultrasonic testing is shown in **Figure 12**. A 10 MHz 0.37-inch diameter - 1-inch focused transducer was used for pulse-echo measurement. A pulser/receiver was connected to the transducer. Pulser/receiver simultaneously transmits and receives the signal. A data acquisition system was used to collect the data. The scan area of the composite plate is shown in **Figure 13**. A 2-inch by 2-inch area was scanned first for detecting the manufacturing damage and flaws in the composite plates. **Figure 14** shows the C-scan image before the impact event. It can be seen clearly from the figure that there are no significant manufacturing defects, damage or flaws in the composite plate. **Figure 15** shows the C-scan image after the high-energy impact event. There are two high-energy impact events at location R1 and R2. A 1-inch by 1-inch area was scanned first for visualizing the defect due to a high-energy impact event. **Figure 15** (a) and (b) shows the evident of impact damage at R1 and R2 location. The size of the impact damage is around 2.5 mm in diameter. From **Figure 15**(a), slight delamination can also be observed around the impact location.

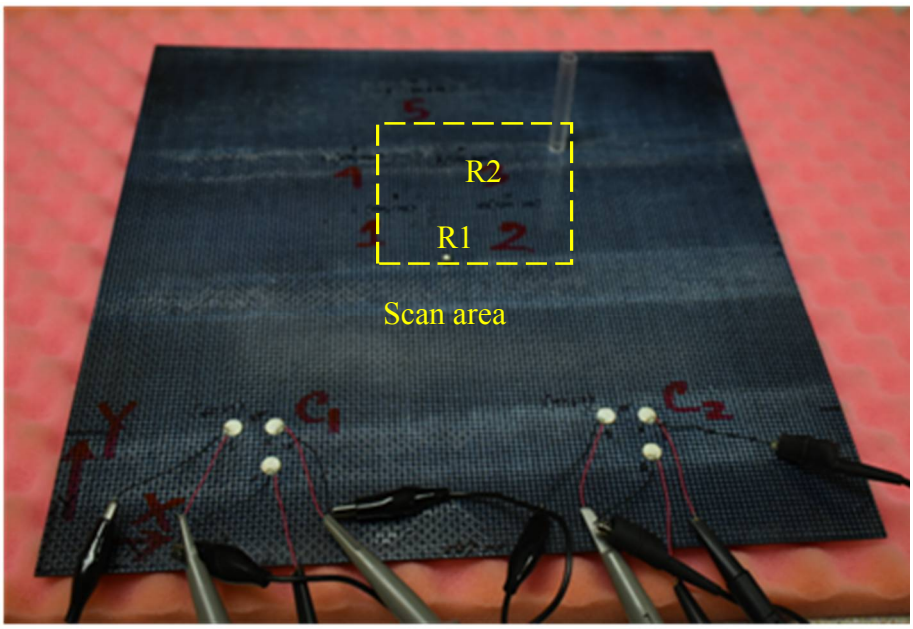

Figure 13. Scan area of the composite plate for immersion ultrasonic inspection

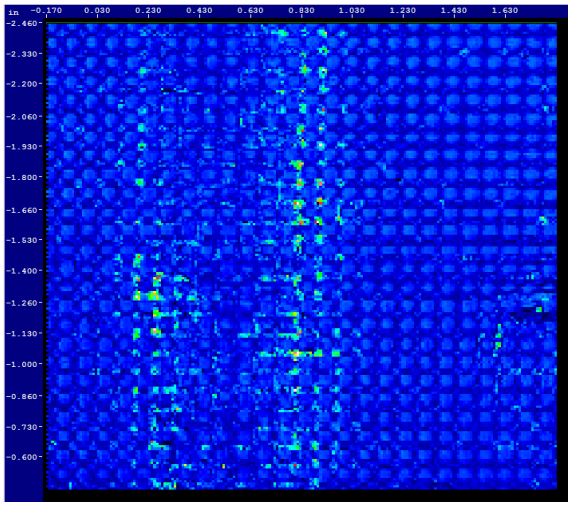

Figure 14. C-scan image of the composite plate for manufacturing defect inspection

Preprints (www.preprints.org) | NOT PEER-REVIEWED | Posted: 7 August 2018 doi:10.20944/preprints201808.0085.v2

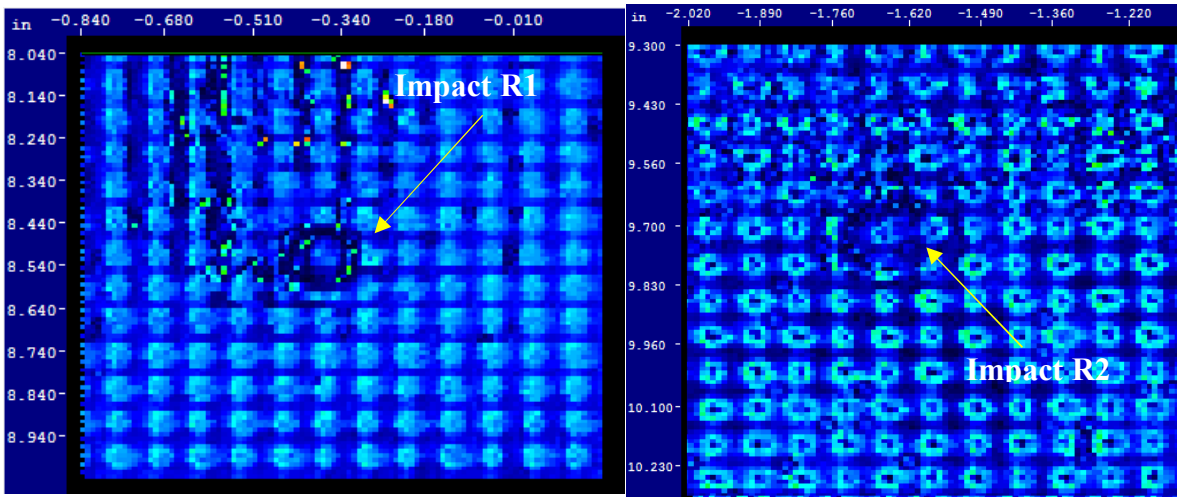

(a) (b)

Figure 15. C-scan image of the composite plate after high-energy impact event (a) impact at R1 location (b) impact at R2 location

5. Conclusions

A compression molding process with a proper cure cycle can be used for manufacturing a composite plate without any significant internal defect. We found that the manufactured plate had a minimal to no defect that can affect the impact detection and localization. Piezoelectric wafer active sensors can be permanently bonded to the composites to detect and localize an impact event. A wavelet transform based signal processing can accurately determine the time of flight of the acoustic signals. The proposed SHM technique can successfully be implemented in practice to monitor impact damage. We found that the experimental measurements are in good agreement with actual impact localization. An immersion ultrasonic scanning method can be used for fast inspection of internal damage in a manufactured plate. There is no significant manufacturing damage was found. After the high-energy impact a clear impact damage was observed in the c-scan image.

Acknowledgment

Support from the National Aeronautics and Space Administration (NASA) and USC McNair center are thankfully acknowledged.

References

1. O. Zabihi, M. Ahmadi, S. Nikafshar, K. Chandrakumar Preyeswary, M. Naebe, A technical review on epoxy-clay nanocomposites: Structure, properties, and their applications in fiber reinforced composites, Compos. Part B Eng. 135 (2018) 1–24. doi:https://doi.org/10.1016/j.compositesb.2017.09.066.
2. L. Molent, C. Forrester, The lead crack concept applied to defect growth in aircraft composite structures, Compos. Struct. 166 (2017) 22–26. doi:https://doi.org/10.1016/j.compstruct.2016.12.076.
3. M.F. Haider, P.K. Majumdar, S. Angeloni, K.L. Reifsnider, Nonlinear anisotropic electrical response of carbon fiber-reinforced polymer composites, J. Compos. Mater. (2017) 21998317719999. doi:10.1177/0021998317719999.
4. Raihan, Rassel, Jon-Michael Adkins, Jeffrey Baker, Fazle Rabbi, and Kenneth Reifsnider. "Relationship of dielectric property change to composite material state degradation." Composites Science and Technology 105 (2014): 160-165.
5. F. Ciampa, M. Meo, A new algorithm for acoustic emission localization and flexural group velocity determination in anisotropic structures, Compos. Part A Appl. Sci. Manuf. 41 (2010) 1777–1786. doi:https://doi.org/10.1016/j.compositesa.2010.08.013.

6. T. Kundu, Acoustic source localization, Ultrasonics. 54 (2014). doi:10.1016/j.ultras.2013.06.009.
7. K.-H. Ip, Y.-W. Mai -, S.S. Kessler, S. Mark Spearing, C. Soutis, Damage detection in composite materials using Lamb wave methods, 2002.
8. V. Giurgiutiu, Structural Health Monitoring with Piezoelectric Wafer Active Sensors (Second Edition), Academic Press, Oxford, 2014. doi:http://dx.doi.org/10.1016/B978-0-12-418691-0.00020-4.
9. X.P. Qing, S.J. Beard, A. Kumar, T.K. Ooi, F.-K. Chang, Built-in Sensor Network for Structural Health Monitoring of Composite Structure, J. Intell. Mater. Syst. Struct. 18 (2006) 39–49. doi:10.1177/1045389X06064353.
10. J.E. Michaels, T.E. Michaels, Guided wave signal processing and image fusion for in situ damage localization in plates, Wave Motion. 44 (2007) 482–492. doi:10.1016/j.wavemoti.2007.02.008.
11. J. Bergman, H. Chung, V. Janapati, I. Li, A. Kumar, S. Kumar-Yadav, D. Chapman, A. Nissan, R. Sarrafi-Nour!, Evaluation of the Real-Time Active Pipeline Integrity Detection System for Corrosion Quantification, Corros. 2016. (2016).
12. A. Tobias, Acoustic-emission source location in two dimensions by an array of three sensors, Non-Destructive Test. 9 (1976) 9–12. doi:https://doi.org/10.1016/0029-1021(76)90027-X.
13. M.Y. Bhuiyan, V. Giurgiutiu, The signatures of acoustic emission waveforms from fatigue crack advancing in thin metallic plates, Smart Mater. Struct. 27 (2017) 1–15. doi:https://doi.org/10.1088/1361-665X/aa9bc2.
14. A. Ebrahimkhanlou, S. Salamone, A probabilistic framework for single-sensor acoustic emission source localization in thin metallic plates, Smart Mater. Struct. 26 (2017) 95026.
15. J. Frieden, J. Cugnoni, J. Botsis, T. Gmür, Low energy impact damage monitoring of composites using dynamic strain signals from FBG sensors – Part I: Impact detection and localization, Compos. Struct. 94 (2012) 438–445. doi:10.1016/J.COMPSTRUCT.2011.08.003.
16. F. Ciampa, M. Meo, Impact detection in anisotropic materials using a time reversal approach, Struct. Heal. Monit. An Int. J. 11 (2012) 43–49. doi:10.1177/1475921710395815.
17. S. Salamone, I. Bartoli, P. Di Leo, F.L. Di Scala, A. Ajovalasit, L. D'Acquisto, J. Rhymer, H. Kim, High-velocity Impact Location on Aircraft Panels Using Macro-fiber Composite Piezoelectric Rosettes, J. Intell. Mater. Syst. Struct. 21 (2010) 887–896. doi:10.1177/1045389X10368450.
18. T. Kundu, S. Das, S.A. Martin, K. V Jata, Locating point of impact in anisotropic fiber reinforced composite plates, Ultrasonics. 48 (2008) 193–201. doi:https://doi.org/10.1016/j.ultras.2007.12.001.
19. J. Jiao, C. He, B. Wu, R. Fei, X. Wang, A new acoustic emission source location technique based on wavelet transform and mode analysis, Front. Mech. Eng. China. 1 (2006) 341–345. doi:10.1007/s11465-006-0006-4.
20. M. Faisal Haider, M.Y. Bhuiyan, B. Poddar, B. Lin, V. Giurgiutiu, Analytical and experimental investigation of the interaction of Lamb waves in a stiffened aluminum plate with a horizontal crack at the root of the stiffener, J. Sound Vib. 431 (2018) 212–225. doi:10.1016/j.jsv.2018.06.018.
21. A. Baghalian, S. Tashakori, V.Y. Senyurek, D. McDaniel, H. Fekrmandi, I.N.. Tansel, Non-Contact Quantification of Longitudinal and Circumferential Defects in Pipes using the Surface Response to Excitation (SuRE) Method, Int. J. Progn. Heal. Manag. 8 (2017) 1–8.
22. A. Migot, V. Giurgiutiu, Impact Localization on a Composite Plate With Unknown Material Properties Using PWAS Transducers and Wavelet Transform, in: ASME Conf. Smart Mater. Adapt. Struct. Intell. Syst., Tampa, FL, 2017: pp. 1–8.
23. T. Kundu, A new technique for acoustic source localization in an anisotropic plate without knowing its material properties, in: 6th Eur. Work. Struct. Heal. Monit., Dresden, Germany, 2012.
24. C.H. Wang, J.T. Rose, F.-K. Chang, A synthetic time-reversal imaging method for structural health monitoring, Smart Mater. Struct. 13 (2004) 415–423. doi:10.1088/0964-1726/13/2/020.
25. Vallen-System, GmbH. (2001), (n.d.). http://www.vallen.de/wavelet/index.html, Munich, Germany.